Quantitative Comparison of ^{124}I PET/CT and ^{131}I SPECT/CT Detectability

Casper Beijst[1,2], Jakob W. Kist[3,4], Mattijs Elschot[1], Max A. Viergever[2], Otto S. Hoekstra[5], Bart de Keizer[1], and Hugo W.A.M. de Jong[1]

[1]Department of Radiology and Nuclear Medicine, UMC Utrecht, Utrecht, The Netherlands; [2]Image Sciences Institute, UMC Utrecht, Utrecht, The Netherlands; [3]Department of Nuclear Medicine, Antoni van Leeuwenhoek Hospital, The Netherlands Cancer Institute, Amsterdam, The Netherlands; [4]Department of Surgical Oncology and Endocrine Surgery, UMC Utrecht, Utrecht, The Netherlands; and [5]Department of Radiology and Nuclear Medicine, VU University Medical Center, Amsterdam, The Netherlands

Radioiodine therapy with ^{131}I is used for treatment of suspected recurrence of differentiated thyroid carcinoma. Pretherapeutic ^{124}I PET/CT with a low activity (~1% of ^{131}I activity) can be performed to determine whether uptake of ^{131}I, and thereby the desired therapeutic effect, may be expected. However, false-negative ^{124}I PET/CT results as compared with posttherapeutic ^{131}I SPECT/CT have been reported by several groups. The purpose of this study was to investigate whether the reported discrepancies may be ascribed to a difference in lesion detectability between ^{124}I PET/CT and ^{131}I SPECT/CT and, hence, whether the administered ^{124}I activity is sufficient to achieve equal detectability. **Methods:** Phantom measurements were performed using the National Electrical Manufacturers Association 2007 image-quality phantom. As a measure of detectability, the contrast-to-noise ratio was calculated. The ^{124}I activity was expressed as the percentage of ^{131}I activity required to achieve the same contrast-to-noise ratio. This metric was defined as the detectability equivalence percentage (DEP). **Results:** Because lower DEPs were obtained for smaller spheres, a relatively low ^{124}I activity was sufficient to achieve similar lesion detectability between ^{124}I PET/CT and ^{131}I SPECT/CT. DEP was 1.5%, 1.9%, 1.9%, 4.4%, 9.0%, and 16.2% for spheres with diameters of 10, 13, 17, 18, 25, and 37 mm, respectively, for attenuation- and scatter-corrected SPECT versus point-spread function (PSF) model–based and time-of-flight (TOF) PET. For no-PSF no-TOF PET, DEP was 3.6%, 2.1%, 3.5%, 7.8%, 15.1%, and 23.3%, respectively. **Conclusion:** A relatively low ^{124}I activity of 74 MBq (~1% of ^{131}I activity) is sufficient to achieve similar lesion detectability between ^{124}I PSF TOF PET/CT and ^{131}I SPECT/CT for small spheres ($\leq$10 mm), since the reported DEPs are close to 1%. False-negative ^{124}I PET/CT results as compared with posttherapeutic ^{131}I SPECT/CT may be ascribed to differences in detectability for large lesions (>10 mm) and for no-PSF no-TOF PET, since DEPs are greater than 1%. On the basis of DEPs of 3.5% for lesion diameters of up to 17 mm on no-PSF no-TOF PET, ^{124}I activities as high as 170 MBq may be warranted to obtain equal detectability.

Key Words: ^{124}I PET/CT; ^{131}I SPECT/CT; detectability; radioiodine; phantom

J Nucl Med 2016; 57:103–108
DOI: 10.2967/jnumed.115.162750

After resection for differentiated thyroid carcinoma, ^{131}I is used as primary treatment to ablate remnant thyroid tissue and potential residual tumor tissue. Treatment with 5.5–7.4 GBq of ^{131}I is indicated if metastases are suspected (*1*). The administered ^{131}I activity is generally empiric and non–patient-specific, since the uptake and hence the therapeutic effectiveness of radioiodine in metastatic lesions is usually not known beforehand. Posttherapeutic ^{131}I SPECT/CT or whole-body scintigraphy is routinely performed to assess tumor uptake. Up to 50% of empirically treated patients show no uptake on posttherapeutic imaging (*2*). To predict whether uptake of radioiodine, and hence a desired therapeutic effect, may be expected, pretherapeutic imaging with a low activity is performed.

Several pretherapeutic imaging strategies have been suggested to optimize patient-specific treatment activity and to prevent unnecessary ^{131}I therapy. ^{131}I whole-body scintigraphy with a low, nontherapeutic ^{131}I activity (half-life, 8 d) can be used for pretherapeutic imaging (*3*). However, diagnostic low-activity ^{131}I scintigraphy does not adequately predict the results of posttherapeutic high-activity ^{131}I scintigraphy (*4*). Moreover, septal penetration by the high-energy (364 and 637 keV) γ-photons negatively affects the image quality of ^{131}I SPECT and scintigraphy, making ^{131}I less suitable for diagnostic purposes. The medium-energy (159 keV) γ-emitter ^{123}I has also been suggested for pretherapeutic imaging, and studies investigating the potential of ^{123}I yielded good results (*5*). However, because of the short half-life of ^{123}I (13.2 h), a large fraction of the administered activity has already decayed before uptake maximizes and imaging is performed.

Alternatively, ^{124}I, with a half-life of 4.2 d, has been proposed for pretherapeutic imaging and assessment of treatment response. Several groups have reported promising results using ^{124}I as a diagnostic agent (*6,7*). ^{124}I is a positron emitter and can be imaged using PET, with resolution, sensitivity, and quantitation superior to those obtainable with the use of ^{131}I in scintigraphy or SPECT. Relatively low activities of 20–74 MBq are used for diagnostic ^{124}I PET imaging (*8–13*).

Unfortunately, clinical experience has shown that ^{124}I PET/CT does not always predict uptake of ^{131}I reliably, and discrepancies between posttherapeutic ^{131}I SPECT/CT and pretherapeutic ^{124}I PET/CT have been reported by several groups (*8–13*). More specifically, in some cases ^{124}I PET/CT images showed no uptake whereas ^{131}I SPECT/CT images did. An example from a study we performed (unpublished data, 2013) is shown in Figure 1 (*14*). These false-negative ^{124}I PET/CT results as compared with ^{131}I SPECT/CT

Received Jun. 30, 2015; revision accepted Oct. 9, 2015.
For correspondence or reprints contact: Casper Beijst, UMC Utrecht, Mail E01.132, P.O. Box 85500, 3508GA Utrecht, The Netherlands.
E-mail: cbeijst@umcutrecht.nl
Published online Oct. 22, 2015.

may be ascribed to a difference in lesion detectability between ^{124}I PET/CT and ^{131}I SPECT/CT.

The purpose of this study was to investigate whether the reported discrepancies may be ascribed to a difference in lesion detectability between ^{124}I PET/CT and ^{131}I SPECT/CT and, hence, whether the administered ^{124}I activity is sufficient to achieve equal detectability. This was done by establishing the ^{124}I activity, expressed as percentage of ^{131}I activity, at which the contrast-to-noise ratio (CNR) was equal for both modalities.

MATERIALS AND METHODS

Phantom

To compare lesion detectability on ^{131}I SPECT/CT and ^{124}I PET/CT images, acquisitions of the International Electrotechnical Commission–National Electrical Manufacturers Association 2007 phantom (PTW Freiburg GmbH) were performed with varying activities. The phantom is torso-shaped and has a lid holding refillable thin-walled spheres 10, 13, 17, 22, 28, and 37 mm in diameter. Separate phantoms were used for the ^{124}I and ^{131}I experiments. The phantoms were filled only once, and different activity concentrations were obtained by leaving the activity to decay. This approach decreases measurement errors in comparison with refilling the phantom. Two phantoms were used for detectability analysis; one with activity in the background compartment and one without.

Clinically, large variations may occur in lesion-to-background ratios. Rubello et al. measured the lesion-to-background ratio with a γ-probe during radioguided surgery and obtained a mean lesion-to-background ratio of 11.4 (*15*). Therefore, we used 2 phantoms with different background concentrations to capture both extremities: no background (1:0) and a high background concentration (10:1). The activity in the spheres ranged from 1.8×10^4 to 4.6 Bq/mL for ^{124}I and from 9.1×10^5 to 3.9×10^2 Bq/mL for ^{131}I. The initial activities are shown in Supplemental Table 1 (supplemental materials are available at http://jnm.snmjournals.org). The activity in the phantoms was chosen such that it could be used to effectively compare lesion detectability in the range around the expected minimum detectable activity (MDA). In total, 45 ^{124}I PET studies were performed over 50 d, and 42 ^{131}I SPECT studies were performed over 90 d.

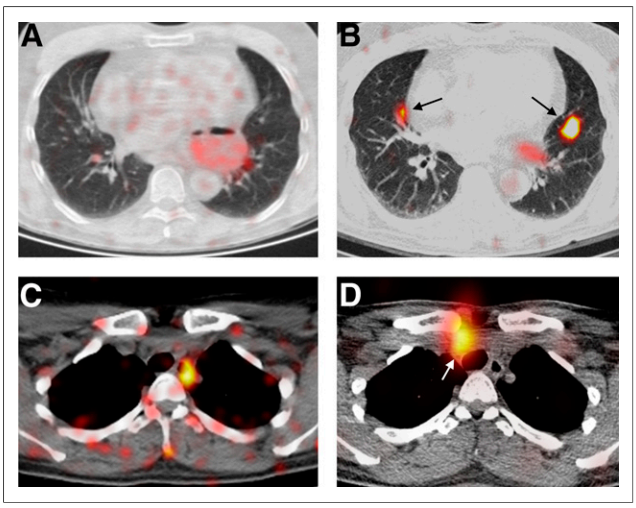

FIGURE 1. Two example THYROPET patients (*14*) in whom ^{124}I PET/CT was false-negative as compared with ^{131}I SPECT/CT. In first patient, ^{124}I PET/CT (A and C) was performed at 2 min per bed position 24 h after oral administration of 74 MBq of ^{124}I using Gemini (Philips) and line-of-response row-action maximum-likelihood reconstruction without TOF correction (no-PSF no-TOF); in second, ^{131}I SPECT/CT (B and D) was performed in 21 min 7 d after oral administration of 7,400 MBq of ^{131}I using Symbia T2 (Siemens) and fast low-angle shot 3-dimensional attenuation-corrected reconstruction (no-SC 6i8s). Arrows indicate metastatic lesions.

Scanners and Acquisitions

A Biograph mCT time-of-flight (TOF) PET/CT scanner (Siemens Healthcare) with TrueV (axial field of view, 21.6 cm) was used to acquire PET data. ^{124}I images were acquired using a 435- to 650-keV energy window at 4 min per bed position, in accordance with the clinical protocol (*14*). Three bed positions were used to ensure that sensitivity was uniform along the entire length of the phantom in the axial direction.

A dual-head Symbia T16 SPECT/CT system (Siemens Healthcare) was used to acquire SPECT data. The BiCore high-energy collimator (Siemens Healthcare) that was used has 8,000 holes, a hole length of 59.7 mm, a hole diameter of 4.0 mm, and septal thickness of 2.0 mm. For all ^{131}I acquisitions, 128 projections were acquired on a 128×128 grid with a 4.8×4.8 mm pixel size. In accordance with the clinical protocol, a 25-s acquisition time per view was used, resulting in a total acquisition time of 26 min.

Reconstruction

PET images were reconstructed to create $200 \times 200 \times 316$ voxel images with a $4.07 \times 4.07 \times 1.50$ mm voxel size. The reconstruction incorporated a ^{124}I prompt γ-correction (*16*) and a randoms correction by adding the gaussian-filtered randoms-sinogram to the forward projection during the iterative reconstruction (*17*). Two reconstruction methods were used to obtain PET images.

The first method was ordered-subset expectation maximization 3-dimensional reconstruction incorporating TOF information (TrueX) with point-spread function (PSF) model–based resolution recovery and CT-based attenuation and scatter correction, using 4 iterations and 21 subsets in accordance with the clinical protocol. A gaussian postreconstruction filter was applied with a full width at half maximum of 5 mm. This method will be referred to as the PSF TOF method.

The second method was ordered-subset expectation maximization 3-dimensional reconstruction with attenuation correction, scatter correction, no TOF modeling, and no PSF model–based resolution recovery. As advised by the vendor, 4 iterations and 24 subsets were used and a gaussian postreconstruction filter was applied with a full width at half maximum of 5 mm. This reconstruction method will be referred to as the no-PSF no-TOF method.

SPECT images were reconstructed to create $128 \times 128 \times 80$ voxel images with a $4.8 \times 4.8 \times 4.8$ mm voxel size. The Siemens fast low-angle shot 3-dimensional reconstruction algorithm was applied, incorporating attenuation correction and resolution recovery using distance-dependent PSFs. Three reconstruction methods were used to obtain SPECT images. The first method used 6 iterations with 8 subsets and triple-energy-window scatter correction (SC 6i8s), the second method used 6 iterations with 8 subsets and did not incorporate scatter correction (no-SC 6i8s), and the third method used 30 iterations with 8 subsets and triple-energy-window scatter correction (SC 30i8s). Reconstruction with 6 iterations and 8 subsets was performed to allow comparison with the clinical trial running at our hospital (*14*), and reconstruction with 30 iterations and 8 subsets was included for increased contrast recovery at the cost of increased image noise (*18,19*).

Quantitative Analysis

Detectability Equivalence Percentage (DEP). As a measure of detectability, we calculated CNR for each sphere using

$$\mathrm{CNR} = \frac{C_H - C_B}{\sigma_B},$$

where C_H is the mean voxel value in the sphere volume of interest (VOI), C_B is the mean voxel value in the background VOI, and σ_B is the SD in the background VOI.

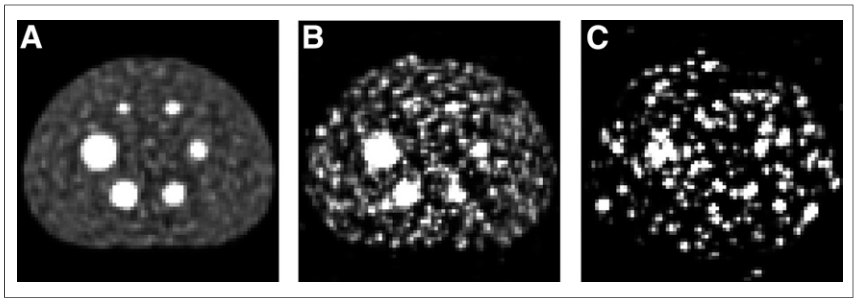

FIGURE 2. Typical ^{124}I PET/CT images of phantom with activity in background compartment reconstructed using PSF TOF method showing central slice through spheres for 2.2×10^4 Bq/mL (A), 9.3×10^2 Bq/mL (B), and 6.5×10^1 Bq/mL (C). Maximum of gray scale is 5 times mean pixel value of image.

Three-dimensional VOI masks were created on the basis of the sphere coordinates determined from the coregistered CT image. The position of the spheres in the CT image was determined automatically using a Hough-transform–based circle detection method (*20*). The background VOI was defined as the entire phantom minus the sphere VOIs. To eliminate the influence of partial-volume effects on the background measurement, a 2-cm margin around the spheres and the phantom edges was subtracted from the background VOI by means of binary erosion.

To assess the difference in sphere detectability between ^{124}I PET/CT and ^{131}I SPECT/CT, ^{124}I activity was expressed as the percentage of ^{131}I activity required to achieve the same CNR. This metric was defined as DEP. For example, a DEP of 1% indicates that the same CNR is obtained on the ^{124}I PET/CT image as on the ^{131}I SPECT/CT image if the ^{124}I activity is 1% of the ^{131}I activity. For each sphere size and sphere-to-background ratio, DEP was determined by calculating the average ratio of the CNR curves (CNR vs. activity) for the 2 isotopes and multiplied by 100 to obtain a percentage. To reduce the influence of noise on the calculated DEPs, regression analysis of the curves was performed. Cubic spline fits of the activity as a function of the sphere CNR were performed and plotted in the log–log domain, because the range of the curves was several orders of magnitude. The mean ratios were calculated over the largest possible interval at which CNR data were acquired for both isotopes and in which CNRs were greater than 1. For the phantom without activity in the background compartment, CNRs for which the mean pixel value of the background VOI was less than 1 were not used for the regression analysis.

MDA. False-negative ^{124}I PET/CT results as compared with ^{131}I SPECT/CT occur when ^{124}I is below MDA and ^{131}I is above MDA. Therefore, MDA was calculated using the Rose criterion (*21*). The Rose criterion states that a lesion is no longer visible when the CNR of the lesion falls below a certain threshold, which can be used to determine the MDA. Because the Rose criterion has been validated for use in 2 dimensions only, we calculated the CNR of the (2-dimensional) central slice through the spheres. The detectability measure K_{2D} was obtained by correcting CNR for lesion size according to

$$K_{2D} = \mathrm{CNR}_{2D} \times \sqrt{N} = \frac{C_{H,2D} - C_{B,2D}}{\sigma_{B,2D}} \times \sqrt{N},$$

where CNR_{2D} is CNR in 2 dimensions, $C_{H,2D}$ is the mean voxel value in the 2-dimensional sphere region of interest (ROI), $C_{B,2D}$ is the mean voxel value in the 2-dimensional background region of interest, $\sigma_{B,2D}$ is the SD in the 2-dimensional background region of interest, and N is the number of pixels in the lesion region of interest. A K_{2D} threshold of 8 was used to determine MDA (*22,23*). MDA was defined as the activity at which the K_{2D}-versus-activity curve intersected with the threshold. Regression analysis of the K_{2D}-versus-activity curves with cubic splines was performed to reduce the influence of noise.

RESULTS

Figures 2 and 3 show typical ^{124}I PET/CT and ^{131}I SPECT/CT National Electrical Manufacturers Association phantom images for different activities. The sphere CNR was calculated and plotted as a function of activity, as shown in Figure 4 and in Supplemental Figures 1 and 2 for the phantom with and without background activity, respectively. Defined as the average ratio between ^{124}I and ^{131}I activity to achieve the same CNR, DEP was calculated for each combination of PET and SPECT reconstruction methods and for each sphere size (Tables 1 and 2).

In general, because lower DEPs were obtained for smaller spheres, a relatively low ^{124}I activity was sufficient to achieve similar lesion detectability between ^{124}I PET/CT and ^{131}I SPECT/CT. Furthermore, DEP depends on reconstruction method. DEP was higher for no-PSF no-TOF PET reconstruction than for PSF TOF reconstruction. Furthermore, DEP was slightly higher for SC 6i8s than for no-SC 6i8s and lower for SC 30i8s than for the other SPECT reconstruction methods. Differences in DEP between PSF TOF and no-PSF no-TOF reconstruction were smaller for the phantom without activity in the background compartment. In general, DEPs were slightly smaller for the phantom without activity in the background compartment.

Table 3 shows the MDA for the phantom with activity in the background compartment. The MDA of ^{124}I was lower for PSF TOF reconstruction than for no-PSF no-TOF reconstruction. Similarly, for the 13- and 17-mm spheres, the MDA of ^{131}I was lower for SC 6i8s than for no-SC 6i8s. However, for the 10-, 22-, and 28-mm spheres, the MDA of ^{131}I was higher for SC 6i8s than for no-SC 6i8s. The MDAs of SC 30i8s were larger than for the other SPECT reconstruction methods.

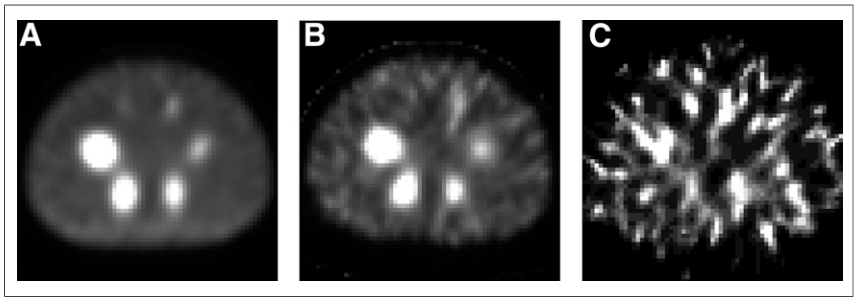

FIGURE 3. Typical ^{131}I SPECT/CT images of phantom with activity in background compartment reconstructed using SC 6i8s method showing central slice through spheres for 9.1×10^5 Bq/mL (A), 4.5×10^4 Bq/mL (B), and 2.2×10^3 Bq/mL (C). Maximum of gray scale is 5 times mean pixel value of image.

DISCUSSION

A relatively low ^{124}I activity of 74 MBq (~1% of ^{131}I activity) was sufficient to achieve similar lesion detectability between

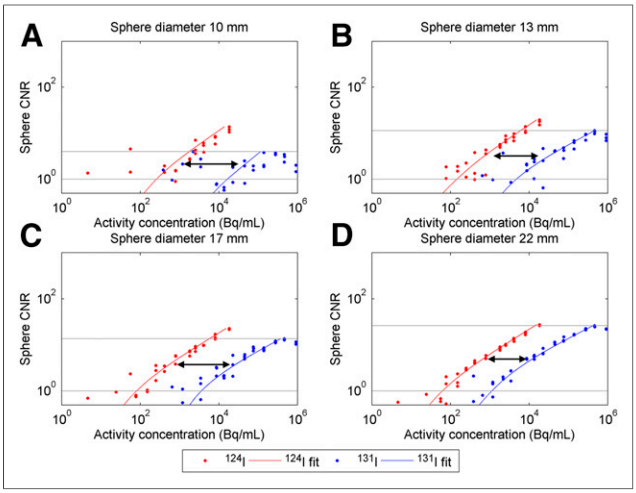

FIGURE 4. Sphere CNR as function of activity for ^{124}I (red) and ^{131}I (blue) phantom with background for spheres with diameters of 10 mm (A), 13 mm (B), 17 mm (C), and 22 mm (D). DEP is determined by calculating ratio of curves, which is graphically represented as horizontal shift of curves (arrows). Gray lines denote interval in which average ratio between curves was determined. Reconstruction was with PSF TOF for PET and SC 6i8s for SPECT.

^{124}I PSF TOF PET/CT and ^{131}I SPECT/CT for small spheres (≤10 mm), since the reported DEPs were close to 1%. False-negative ^{124}I PET/CT results as compared with posttherapeutic ^{131}I SPECT/CT may be ascribed to differences in detectability for large lesions (>10 mm) and for no-PSF no-TOF PET since DEPs were greater than 1%.

The results showed that DEP was lower for smaller spheres, indicating that smaller spheres are relatively more easily detected on PET than on SPECT. This can be explained by the fact that the resolution of ^{124}I PET images (~5 mm) generally is higher than that of ^{131}I SPECT images (~15 mm). Therefore, differences in CNR are large in spheres that measure between 5 and 15 mm.

Activities frequently used in clinical practice and studies are 74 MBq of ^{124}I and 7,400 MBq of ^{131}I; thus, the administered ^{124}I activity is approximately 1% of the administered ^{131}I activity. However, because different scan delays are used after administration, it is necessary to correct for physical decay during the delay. The ^{124}I PET and the ^{131}I SPECT acquisitions are usually performed 24 h and 7 d after administration, respectively, so that at scanning time the ^{124}I activity is approximately 1.5% of the ^{131}I activity if we correct for physical decay. Tables 1 and 2 show that

TABLE 1
DEPs for Phantom with Background

Reconstruction method		Millimeters					
PET	SPECT	10	13	17	22	28	37
PSF TOF	SC 6i8s	1.5	1.9	1.9	4.4	9.0	16.2
No-PSF no-TOF	SC 6i8s	3.6	2.1	3.5	7.8	15.1	23.3
PSF TOF	no-SC 6i8s	1.4	2.1	1.9	4.1	6.8	11.6
No-PSF no-TOF	no-SC 6i8s	3.4	2.1	3.6	7.4	11.9	18.1
PSF TOF	SC 30i8s	0.8	1.3	1.0	1.7	2.1	2.7
No-PSF no-TOF	SC 30i8s	1.8	1.5	2.0	2.8	3.4	3.9

TABLE 2
DEPs for Phantom Without Background

Reconstruction method		Millimeters					
PET	SPECT	10	13	17	22	28	37
PSF TOF	SC 6i8s	1.1	2.3	3.3	4.8	5.9	7.0
No-PSF no-TOF	SC 6i8s	1.7	3.2	3.2	4.2	4.8	5.5
PSF TOF	no-SC 6i8s	0.8	1.4	2.0	2.9	4.1	4.3
No-PSF no-TOF	no-SC 6i8s	1.3	2.6	2.6	3.3	4.2	4.0
PSF TOF	SC 30i8s	0.9	1.1	1.4	1.6	1.7	1.8
No-PSF no-TOF	SC 30i8s	1.4	1.7	1.6	1.6	1.7	1.7

for some sphere sizes and reconstruction algorithms, DEP is less than 1.5%. Therefore, for small spheres (≤10 mm) on PSF TOF PET, a 74-MBq ^{124}I activity is sufficient to achieve similar detectability between low-activity ^{124}I PET/CT and high-activity ^{131}I SPECT/CT. This shows that false-negative results on low-activity ^{124}I PSF TOF PET/CT, as compared with posttherapeutic high-activity ^{131}I SPECT/CT, are not likely caused by differences in the detectability of small lesions. A significant number of lesions seen in clinical practice are expected to be smaller than 10 mm (*24*). For larger lesions (>10 mm) and no-PSF no-TOF PET, DEP generally is greater than 1.5%, and a 74-MBq ^{124}I activity is not sufficient to achieve similar detectability between low-activity ^{124}I PET/CT and high-activity ^{131}I SPECT/CT. Reported discrepancies, such as the example shown in Figure 1, may therefore be caused by differences in detectability.

The administered ^{124}I activity is a factor that should be considered when our results are compared with those of other studies. Several clinical studies have been performed with ^{124}I activities lower than 74 MBq (*8,9,11*). The probability of a false-negative ^{124}I PET/CT result as compared with posttherapeutic ^{131}I SPECT/CT considerably increases with lower ^{124}I activities. When 25 MBq of ^{124}I and 7,400 MBq of ^{131}I are administered, the ratio of ^{124}I to ^{131}I activity is approximately 0.5% when corrected for physical decay. Since this is lower than the reported DEPs, discrepancies are more likely to occur as a result of differences in detectability.

An activity of 90 MBq is sufficient to achieve similar detectability for lesion diameters of up to 17 mm on PSF TOF PET, with DEPs up to 1.8%. On the basis of DEPs of 3.5% for lesion diameters of up to 17 mm on no-PSF no-TOF PET, ^{124}I activities as high as 170 MBq may be warranted to obtain equal detectability. However, a limiting factor for high pretherapeutic activities may be thyroid stunning, although stunning due to ^{124}I is controversial, and the origin and existence of stunning still are a hotly debated issue (*25*).

Discrepancies between ^{124}I and ^{131}I distribution in tissue as a consequence of differences in uptake and washout may be influenced by additional factors not assessed in this study. First, unlike phantoms, thyroid tumors or thyroid cancer metastases are inhomogeneous structures consisting of cancer cells, blood vessels, and connective tissue with different iodine concentrations, inducing partial-volume effects that may affect the measured contrast. Second, iodine uptake may be influenced by whether patients are prepared using thyroid hormone withdrawal or using recombinant human thyroid-stimulating hormone stimulation of iodine uptake. Third, cell damage as a consequence of delivered dose of activity may influence retention time and therefore cause differences in physiologic washout properties between ^{124}I and ^{131}I. Washout of

TABLE 3
MDAs for Phantom with Background

Isotope	Reconstruction method	Bq/mL					
		10	13	17	22	28	37
^{124}I	PSF TOF	1.0×10^3	4.1×10^2	1.6×10^2	8.3×10^1	4.4×10^1	2.1×10^1
^{124}I	No-PSF no-TOF	3.0×10^3	5.1×10^2	3.0×10^2	1.9×10^2	8.6×10^1	4.6×10^1
^{131}I	SC 6i8s	1.1×10^5	2.2×10^4	8.2×10^3	1.7×10^3	6.5×10^2	
^{131}I	No-SC 6i8s	9.6×10^4	2.5×10^4	8.9×10^3	1.4×10^3	4.2×10^2	
^{131}I	SC 30i8s	1.9×10^5	3.3×10^4	1.5×10^4	4.2×10^3	2.0×10^3	

^{131}I is expected to be faster in damaged cells (*24*). Fourth, the contrast of ^{131}I lesions may increase when scanning is delayed: background activity may clear more quickly than tumor activity, and contrast in the images may therefore, contraintuitively, increase over time (*10*). In clinical practice, one of the few adjustable parameters that influence activity is the delay between administration and acquisition. However, the timing of the ^{131}I SPECT/CT acquisition still is a matter of debate in the literature. In fact, Salvatori et al. stated that "perfect timing" probably does not exist because of differences in ^{131}I kinetics in different patients and in different metastases (*26*). A delay of 7 d for this study was chosen to allow washout of background activity (*27*). Similar to ^{131}I, ^{124}I uptake differs significantly among metastases, although peak uptake is generally observed about 24 h after administration (*28,29*). Therefore, a delay of 24 h was used for the ^{124}I PET/CT acquisition.

The purpose of this study was not to investigate the impact of physiologic factors but to quantitatively compare lesion detectability on ^{124}I PET/CT and ^{131}I SPECT/CT images. It may not be accurate to assume that physical decay is the only factor affecting the ratio of ^{124}I to ^{131}I activity, and interpretation of the results depends on this assumption. However, the measured DEPs do not depend on physiologic factors. To our knowledge, phantom measurements that compare the detectability of ^{124}I and ^{131}I quantitatively have not been published before.

CNR values lower than 1 were not used for the regression analysis and calculation of DEP. These values are inherently noisy because of the low number of counts. Furthermore, rounding errors occurred through conversion to the DICOM format when the mean voxel value in the background compartment was lower than 1. Consequently, for low activities in the phantom without background activity, SD in the background compartment was underestimated and CNR overestimated. Therefore, these data points (mean background VOI < 1) were not used to determine DEPs and MDAs.

Diagnostic ^{131}I SPECT/CT with 37–150 MBq of ^{131}I can also be performed for pretherapeutic imaging (*3*). However, this study showed that false-negative diagnostic scans as compared with posttherapeutic scans may be ascribed to the difference in administered activity and that false-negative results are likely, especially for smaller lesions with high MDAs.

False-negative ^{124}I PET/CT results as compared with ^{131}I SPECT/CT occur when ^{124}I is below MDA and ^{131}I is above MDA. The MDAs of ^{131}I and ^{124}I were therefore determined for the different reconstruction methods. The MDA of ^{131}I was higher for SC 6i8s reconstruction than for no-SC 6i8s reconstruction for some sphere sizes (10, 22, and 28 mm). MDAs were not necessarily lower for images obtained with scatter correction, possibly because of the additional noise introduced in the reconstruction by the scatter projections. Unfortunately, no ^{131}I MDAs could be obtained for the 37-mm spheres because not enough data were available for low CNRs.

DEPs were lower for 30i8s than for 6i8s SPECT reconstruction, because generally lower CNRs were obtained for 30i8s than for 6i8s. The cause was the increase in background noise with number of iterations, which lowered CNR. Therefore, the ^{124}I activity expressed as a percentage of ^{131}I activity required to achieve the same CNR (i.e., DEP) was lower for 30i8s than for 6i8s.

On the basis of the coregistered CT data, the sizes of the lesions in Figure 1 are 5 and 7 mm (Fig. 1B) and 12 mm (Fig. 1D). DEP for the 10-mm sphere was between 1.3 and 3.4, depending of the lesion-to-background ratio (Tables 1 and 2), so that a relatively low ^{124}I activity of 74 MBq ($\sim$1% of ^{131}I activity) may not be sufficient to achieve similar detectability. The false-negative ^{124}I PET/CT results as compared with ^{131}I SPECT/CT may therefore be ascribed to differences in detectability. Unfortunately, no DEPs were calculated for sphere diameters smaller than 10 mm. In general, discrepancies between ^{124}I PET/CT and ^{131}I SPECT/CT depend on many factors, and this study showed that the dose of ^{124}I activity should be chosen carefully.

CONCLUSION

A relatively low ^{124}I activity of 74 MBq ($\sim$1% of ^{131}I activity) is sufficient to achieve similar lesion detectability between ^{124}I PSF TOF PET/CT and ^{131}I SPECT/CT for small spheres ($\leq$10 mm), since the reported DEPs are close to 1%. A ^{124}I activity of 90 MBq is sufficient to achieve similar detectability for lesion diameters of up to 17 mm on PSF TOF PET, with DEPs of up to 1.8%. False-negative ^{124}I PET/CT results as compared with posttherapeutic high-activity ^{131}I SPECT/CT may be ascribed to differences in detectability for large lesions ($>$10 mm) and for no-PSF no-TOF PET, since DEPs are greater than 1%. On the basis of DEPs of 3.5% for lesion diameters of up to 17 mm on no-PSF no-TOF PET, ^{124}I activities as high as 170 MBq may be warranted to obtain equal detectability.

DISCLOSURE

The costs of publication of this article were defrayed in part by the payment of page charges. Therefore, and solely to indicate this fact, this article is hereby marked "advertisement" in accordance with 18 USC section 1734. No potential conflict of interest relevant to this article was reported.

ACKNOWLEDGMENT

We thank Dr. Dennis Brian Martin Dickerscheid for providing the phantom.

REFERENCES

1. Luster M, Clarke SE, Dietlein M, et al. Guidelines for radioiodine therapy of differentiated thyroid cancer. *Eur J Nucl Med Mol Imaging.* 2008;35:1941–1959.
2. Ma C, Xie J, Kuang A. Is empiric ^{131}I therapy justified for patients with positive thyroglobulin and negative ^{131}I whole-body scanning results? *J Nucl Med.* 2005;46:1164–1170.
3. Pacini F, Lippi F, Formica N, et al. Therapeutic doses of iodine-131 reveal undiagnosed metastases in thyroid cancer patients with detectable serum thyroglobulin levels. *J Nucl Med.* 1987;28:1888–1891.
4. Pacini F, Agate L, Elisei R, et al. Outcome of differentiated thyroid cancer with detectable serum Tg and negative diagnostic ^{131}I whole body scan: comparison of patients treated with high ^{131}I activities versus untreated patients. *J Clin Endocrinol Metab.* 2001;86:4092–4097.
5. Urhan M, Dadparvar S, Mavi A, et al. Iodine-123 as a diagnostic imaging agent in differentiated thyroid carcinoma: a comparison with iodine-131 post-treatment scanning and serum thyroglobulin measurement. *Eur J Nucl Med Mol Imaging.* 2007;34:1012–1017.
6. Erdi YE, Macapinlac H, Larson SM, et al. Radiation dose assessment for I-131 therapy of thyroid cancer using I-124 PET imaging. *Clin Positron Imaging.* 1999;2:41–46.
7. Freudenberg LS, Antoch G, Jentzen W, et al. Value of ^{124}I-PET/CT in staging of patients with differentiated thyroid cancer. *Eur Radiol.* 2004;14:2092–2098.
8. de Pont C, Halders S, Bucerius J, Mottaghy F, Brans B. ^{124}I PET/CT in the pretherapeutic staging of differentiated thyroid carcinoma: comparison with posttherapy ^{131}I SPECT/CT. *Eur J Nucl Med Mol Imaging.* 2013;40:693–700.
9. Freudenberg LS, Jentzen W, Müller SP, Bockisch A. Disseminated iodine-avid lung metastases in differentiated thyroid cancer: a challenge to ^{124}I PET. *Eur J Nucl Med Mol Imaging.* 2008;35:502–508.
10. Khorjekar GR, Van Nostrand D, Garcia C, et al. Do negative ^{124}I pretherapy positron emission tomography scans in patients with elevated serum thyroglobulin levels predict negative ^{131}I posttherapy scans? *Thyroid.* 2014;24:1394–1399.
11. Lammers GK, Esser JP, Pasker PC, Sanson-van Praag ME, de Klerk JM. Can I-124 PET/CT predict pathological uptake of therapeutic dosages of radioiodine (I-131) in differentiated thyroid carcinoma? *Adv J Mol Imaging.* 2014;4:27–34.
12. Phan HT, Jager P, Paans AJ, et al. The diagnostic value of ^{124}I-PET in patients with differentiated thyroid cancer. *Eur J Nucl Med Mol Imaging.* 2008;35:958–965.
13. Van Nostrand D, Moreau S, Bandaru VV, et al. ^{124}I positron emission tomography versus ^{131}I planar imaging in the identification of residual thyroid tissue and/or metastasis in patients who have well-differentiated thyroid cancer. *Thyroid.* 2010;20:879–883.
14. Kist JW, de Keizer B, Stokkel MPM, Hoekstra OS, Vogel WV; THYROPET study group. Recurrent differentiated thyroid cancer: towards personalized treatment based on evaluation of tumor characteristics with PET (THYROPET study): study protocol of a multicenter observational cohort study. *BMC Cancer.* 2014;14:405.
15. Rubello D, Salvatori M, Ardito G, et al. Iodine-131 radio-guided surgery in differentiated thyroid cancer: outcome on 31 patients and review of the literature. *Biomed Pharmacother.* 2007;61:477–481.
16. Preylowski V, Schlogl S, Schoenahl F, et al. Is the image quality of I-124-PET impaired by an automatic correction of prompt gammas? *PLoS One.* 2013;8: e71729.
17. Willowson KP, Tapner M; QUEST investigator team, Bailey DL. A multicentre comparison of quantitative ^{90}Y PET/CT for dosimetric purposes after radioembolization with resin microspheres : the QUEST phantom study. *Eur J Nucl Med Mol Imaging.* 2015;42:1202–1222.
18. Dewaraja YK, Frey EC, Sgouros G, et al. MIRD pamphlet no. 23: quantitative SPECT for patient-specific 3-dimensional dosimetry in internal radionuclide therapy. *J Nucl Med.* 2012;53:1310–1325.
19. Dewaraja YK, Ljungberg M, Green AJ, et al. MIRD pamphlet no. 24: guidelines for quantitative ^{131}I SPECT in dosimetry applications. *J Nucl Med.* 2013;54:2182–2188.
20. Duda RO, Hart PE. Use of the Hough transformation to detect lines and curves in pictures. *Commun ACM.* 1972;15:11–15.
21. Rose A. The sensitivity performance of the human eye on an absolute scale. *J Opt Soc Am.* 1948;38:196–208.
22. Bright DS, Newbury DE, Steel EB. Visibility of objects in computer simulations of noisy micrographs. *J Microsc.* 1998;189:25–42.
23. Carlier T, Eugène T, Bodet-Milin C, et al. Assessment of acquisition protocols for routine imaging of Y-90 using PET/CT. *EJNMMI Res.* 2013;3:11.
24. Jentzen W, Hoppenbrouwers J, van Leeuwen P, et al. Assessment of lesion response in the initial radioiodine treatment of differentiated thyroid cancer using ^{124}I PET imaging. *J Nucl Med.* 2014;55:1759–1765.
25. McDougall IR, Iagaru A. Thyroid stunning: fact or fiction? *Semin Nucl Med.* 2011;41:105–112.
26. Salvatori M, Perotti G, Villani MF, et al. Determining the appropriate time of execution of an I-131 post-therapy whole-body scan: comparison between early and late imaging. *Nucl Med Commun.* 2013;34:900–908.
27. Chong A, Song H-C, Min J-J, et al. Improved detection of lung or bone metastases with an I-131 whole body scan on the 7th day after high-dose I-131 therapy in patients with thyroid cancer. *Nucl Med Mol Imaging.* 2010;44:273–281.
28. Jentzen W, Freudenberg L, Eising EG, Sonnenschein W, Knust J, Bockisch A. Optimized ^{124}I PET dosimetry protocol for radioiodine therapy of differentiated thyroid cancer. *J Nucl Med.* 2008;49:1017–1023.
29. Pettinato C, Spezi E, Nanni C, et al. Pretherapeutic dosimetry in patients affected by metastatic thyroid cancer using ^{124}I PET/CT sequential scans for ^{131}I treatment planning. *Clin Nucl Med.* 2014;39:e367–e374.